Developmental Cell
Article

Germline Quality Control: eEF2K Stands Guard to Eliminate Defective Oocytes

Hsueh-Ping Chu,[1,6] Yi Liao,[1,6] James S. Novak,[1,6] Zhixian Hu,[1] Jason J. Merkin,[1] Yuriy Shymkiv,[1] Bart P. Braeckman,[2] Maxim V. Dorovkov,[1] Alexandra Nguyen,[1] Peter M. Clifford,[3] Robert G. Nagele,[3] David E. Harrison,[4] Ronald E. Ellis,[5] and Alexey G. Ryazanov[1,*]

[1]Department of Pharmacology, Rutgers The State University of New Jersey, Robert Wood Johnson Medical School, Piscataway, NJ 08854, USA
[2]Department of Biology, University of Gent, 9000 Gent, Belgium
[3]Department of Cell Biology, Rowan University School of Osteopathic Medicine, Stratford, NJ 08084, USA
[4]The Jackson Laboratory, Bar Harbor, ME 04609, USA
[5]Department of Molecular Biology, Rowan University School of Osteopathic Medicine, Stratford, NJ 08084, USA
[6]These authors contributed equally to this work
*Correspondence: ryazanag@rutgers.edu
http://dx.doi.org/10.1016/j.devcel.2014.01.027

SUMMARY

The control of germline quality is critical to reproductive success and survival of a species; however, the mechanisms underlying this process remain unknown. Here, we demonstrate that elongation factor 2 kinase (eEF2K), an evolutionarily conserved regulator of protein synthesis, functions to maintain germline quality and eliminate defective oocytes. We show that disruption of eEF2K in mice reduces ovarian apoptosis and results in the accumulation of aberrant follicles and defective oocytes at advanced reproductive age. Furthermore, the loss of eEF2K in *Caenorhabditis elegans* results in a reduction of germ cell death and significant decline in oocyte quality and embryonic viability. Examination of the mechanisms by which eEF2K regulates apoptosis shows that eEF2K senses oxidative stress and quickly downregulates short-lived antiapoptotic proteins, XIAP and c-FLIP$_L$ by inhibiting global protein synthesis. These results suggest that eEF2K-mediated inhibition of protein synthesis renders cells susceptible to apoptosis and functions to eliminate suboptimal germ cells.

INTRODUCTION

Germline transmission across generations without the accumulation of deleterious genetic defects remains an intriguing and fundamental biological question. One hypothesis suggests that germline selection via apoptosis may play a role in the elimination of defective germ cells. Female mammals generate millions of primordial oogonia but ovulate only a few hundred mature oocytes throughout their reproductive lifespans. The postnatal loss of oocytes is due to follicle degeneration (atresia), which is driven by apoptosis of either the germ cell or somatic (granulosa) cell lineage in mammals (Tilly, 2001). Recent studies have reported that mutations inhibiting cell death result in a severe decline in oocyte quality in *Caenorhabditis elegans* (Andux and Ellis, 2008), suggesting that regulation of apoptosis plays an important role in the control of female germ cell quality. However, the mechanisms regulating the decision between germ cell survival and death remain unknown. Here, we report a mechanism by which inhibition of protein synthesis by eEF2K regulates this decision-making process and eliminates defective oocytes in the female germline.

eEF2 kinase (eEF2K) is a regulator of protein synthesis that specifically phosphorylates eukaryotic elongation factor 2 (eEF2). eEF2 functions to promote ribosomal translocation, the reaction that results in the movement of the ribosome along the mRNA during protein synthesis. eEF2 is one of the most prominently phosphorylated proteins observed in cell lysates and is the apparent exclusive substrate for eEF2 kinase (Ryazanov et al., 1988). Phosphorylation of eEF2 by eEF2K arrests mRNA translation and constitutes a critical mechanism for the regulation of global protein synthesis (Ryazanov et al., 1988).

eEF2K is highly conserved among eukaryotes from mammals to invertebrates (Ryazanov, 2002), with human and mouse eEF2K sharing 99% overall amino acid identity. In addition, the *C. elegans* homolog, EFK-1, also shares ~90% homology with mouse and human eEF2K in both the N-terminal alpha-kinase domain and C-terminal eEF2-targeting domain. Furthermore, eEF2 and the site of phosphorylation by eEF2K are also conserved among these organisms, suggesting that the regulation of eEF2 by eEF2K is an evolutionarily conserved mechanism to regulate protein synthesis. eEF2K activity is Ca^{2+}/calmodulin-dependent, affected by cellular pH, stresses (Patel et al., 2002; White et al., 2007), and nutrients (Browne and Proud, 2002) and may help tumor cells adapt to nutrient deprivation (Leprivier et al., 2013). Previous studies of eEF2K were mainly performed in cell culture or cell lysates, however, the activity of eEF2K in vivo had not been well-studied and the physiological role of eEF2K had remained unknown.

Here, we investigated the physiological role of eEF2K in both mice and *C. elegans.* As the result of extensive immunostaining of phosphorylated eEF2 in various mouse tissues and *C. elegans*, we discovered that the highest activity of eEF2K occurs specifically in the female gonads of these organisms. Furthermore, genetic knockout of eEF2K in mice and

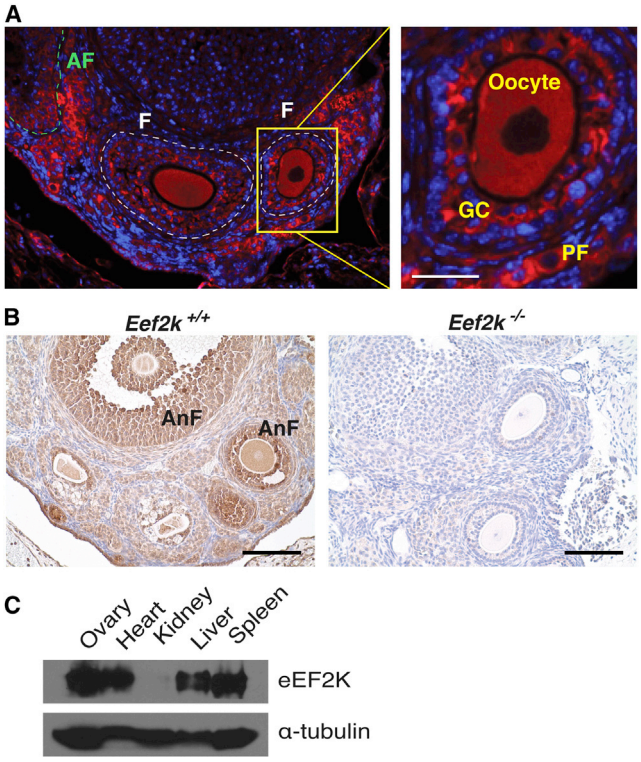

Figure 1. Intense Phosphorylation of eEF2 in Mouse Ovaries

(A) Immunofluorescent staining of p-eEF2 in *Eef2K*$^{+/+}$ mouse ovary. Scale bars represent 25 μm. F, developing follicle; AF, atretic follicle; PF, primordial follicle; GC, granulosa cells. Red, p-eEF2 staining; blue, DAPI staining.

(B) Immunohistochemical staining of p-eEF2 in *Eef2K*$^{+/+}$ and *Eef2K*$^{-/-}$ mouse ovaries. Scale bars represent 100 μm. AnF, antral follicle. Brown, p-eEF2 staining; blue, Hematoxylin staining.

(C) The levels of eEF2K protein in various mouse tissues lysates by western blot analysis. eEF2K is strongly expressed in the mouse ovaries.

See also Figure S1.

C. elegans revealed that its function in the germline is to facilitate apoptosis and maintain oocyte quality. We then further examined the role of eEF2K during apoptosis and found that it is required for inhibition of protein synthesis and downregulation of short-lived antiapoptotic proteins. These results suggest that eEF2K renders cells more susceptible to apoptosis and may constitute a key component of a conserved mechanism to maintain germline quality.

RESULTS

Phosphorylation of eEF2 by eEF2K Occurs Primarily in the Ovaries of Mice

To investigate the physiological role of eEF2K, we examined where eEF2K was most active in the mouse by immunostaining of phosphorylated eEF2 (p-eEF2) in various mouse tissues. While we detected limited staining in lymph nodes, small intestine, and testes, the most intense p-eEF2 staining was observed in mouse ovaries. In fact, p-eEF2 was detected in all types of follicles including primordial, primary, preantral, antral, and atretic follicles (Figures 1A and 1B and Figure S1E available online). Phosphorylation of eEF2 was localized to the granulosa cells, oocytes, and luteal cells (Figures 1A and S1A), but not detected in interfollicular stromal cells (Figure S1B), indicating that eEF2K is activated specifically during folliculogenesis (Figures 1A and 1B). The spatial distribution and intensity of p-eEF2 in the mouse ovary is summarized in Figure S1E. The highest activity of eEF2K was found in the inner layer of granulosa cells that closely surround the oocytes of developing follicles (Figures 1A and 1B). In addition, p-eEF2 was also present in the granulosa cells and dying oocytes of atretic follicles, which were identified by hematoxylin or DAPI staining (Figures S1C and S1D). Consistent with eEF2K activity, the protein expression of eEF2K is highest in ovaries among those tissues that had been investigated (Figure 1C).

Knockout of eEF2K Leads to Increase in Abnormal Antral Follicles and Unhealthy Oocytes at Advanced Age

To uncover the physiological function of eEF2K, we created a homozygous *Eef2K* knockout mouse (Figures S2A–S2E). The *Eef2K*$^{-/-}$ animals were viable and phenotypically normal in most aspects examined (Figures S2F–S2I; Supplemental Experimental Procedures). Unexpectedly, we found that while the ovaries of postmenopausal-aged wild-type mice exhibited no follicles (Figure 2A), the ovaries of 20-month-old *Eef2K*$^{-/-}$ mice contained follicles at various developmental stages and corpora lutea (Figure 2A). Further investigation revealed that 88% of 17- to 21-month-old *Eef2K*$^{-/-}$ ovaries still possessed large antral follicles with oocytes, while antral follicles were only present in 33% of age-matched *Eef2K*$^{+/+}$ ovaries ($p = 0.015$; Figure S2J). Although *Eef2K*$^{-/-}$ aged ovaries possessed more antral follicles, many of them contained an unhealthy-looking, irregular-shaped oocyte (Figures 2B, and S2K–S2N). In addition, many of the aged *Eef2K*$^{-/-}$ ovaries exhibited several preovulatory-like follicles with a diameter of over 500 μm (Figure 2C), which were not observed in the aged-matched wild-type females. Mitotic features such as chromosomal alignment along the metaphase plate were found in granulosa cells of these preovulatory-like follicles from *Eef2K*$^{-/-}$ ovaries (Figure 2C), and we found that <0.1% of the granulosa cells in these ovaries displayed pyknotic nuclei. These results suggest that the preovulatory-like follicles in *Eef2K*$^{-/-}$ ovaries were still growing despite the presence of an unhealthy oocyte, or the absence of one altogether. Moreover, 20-month-old *Eef2K*$^{-/-}$ females displayed hypertrophy of uterine tissue (Figure 2D). Taken together, our observations of *Eef2K*$^{-/-}$ females of advanced reproductive age suggest that eEF2K functions in follicle degeneration and affects the regulation of apoptosis in ovaries.

Knockout of eEF2K Reduces Apoptosis in Mouse Ovary

The accumulation of follicles in aged *Eef2K*$^{-/-}$ ovaries led us to investigate the role of eEF2K in follicular apoptosis. To analyze follicular atresia in *Eef2K*$^{-/-}$ mice, we quantified pyknotic nuclei in granulosa cells of antral follicles. The histology of serial ovarian sections from 6-month-old mice revealed a significant reduction of pyknosis in the antral follicles of *Eef2K*$^{-/-}$ mice (Figures 3A and 3B). In addition, we monitored apoptosis by measuring levels of cleaved caspase-3 by immunohistochemistry of ovarian sections of 2-month-old mice and observed that the *Eef2K*$^{-/-}$ ovaries exhibited a significant decrease of cleaved caspase-3 positive cells in estrus phase (Figure 3C) and a slight decrease

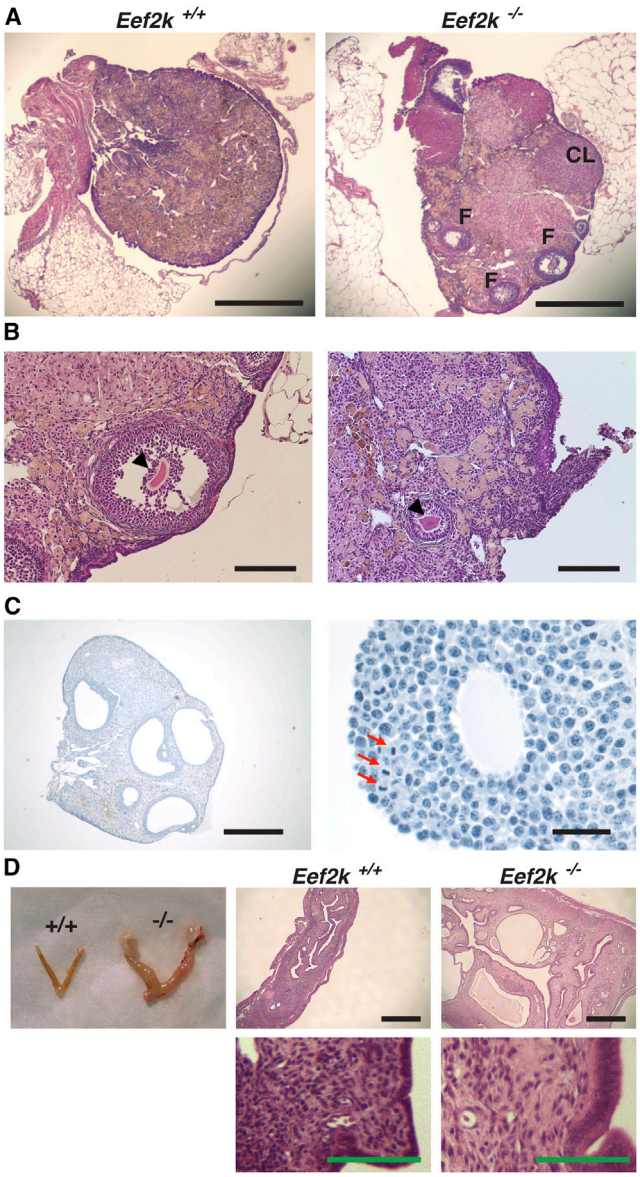

Figure 2. Knockout of eEF2K Preserves Follicles and Reduces Oocyte Quality in Aged Female Mice

(A) Hematoxylin and eosin staining of 20-month-old mouse ovary sections. Scale bars represent 500 μm. F, follicle; CL, corpus luteum.

(B) Hematoxylin and eosin staining of antral follicle (left panel) with an unhealthy, sickle-shaped oocyte (arrowhead), and preantral follicle (right panel) with an unhealthy oocyte with blebs (arrowhead) from 20-month-old *Eef2K*$^{-/-}$ mice. Scale bars represent 100 μm.

(C) Iron hematoxylin/aniline blue staining of ovary from 17-month-old *Eef2K*$^{-/-}$ mouse. Left panel: preovulatory-like follicles with a diameter >500 μm in the *Eef2K*$^{-/-}$ ovary. Scale bars represent 500 μm. Right panel: preovulatory-like follicles contain granulosa cells undergoing mitosis. Red arrows indicate granulosa cells in metaphase of the cell cycle. Scale bars represent 25 μm.

(D) Dissected uterus and hematoxylin and eosin staining of uterine tissue from 20-month-old *Eef2K*$^{+/+}$ and *Eef2K*$^{-/-}$ mice. Black scale bars represent 500 μm; green scale bars represent 50 μm.

See also Figures S2, S3, and Supplemental Experimental Procedures.

during proestrus phase (Figure 3C). The activated caspase-3 staining was mostly localized to the inner layers of granulosa cells of the developing follicle, similar to where we observed the most intense phosphorylation of eEF2 (Figures 1A, 1B, and 3D). Furthermore, although examination of cell morphology in vaginal smears of *Eef2K*$^{+/+}$ and *Eef2K*$^{-/-}$ mice show no detectable differences (Figure S3A), the estrus stage is significantly prolonged in *Eef2K*$^{-/-}$ mice (Figure S3B, $p = 0.002$), leading to an increase in the duration of estrous cycle. While there is no difference in the hormone levels of follicle-stimulating hormone (FSH), luteinizing hormone (LH), or estradiol in estrus phase, the level of progesterone is slightly higher in *Eef2K*$^{-/-}$ mice, although not statistically significant (Figure S3J, $p = 0.08$).

It has been reported that inhibition of protein synthesis sensitizes cells to tumor necrosis factor alpha (TNF-α)-induced apoptosis (Kreuz et al., 2001; Micheau et al., 2001; Wang et al., 2008). We further investigated whether eEF2K mediates granulosa cell death induced by TNF-α in cultured cells. Granulosa cells were isolated from wild-type and *Eef2K*$^{-/-}$ mice and incubated in the presence of TNF-α with or without cycloheximide. We found that granulosa cells from *Eef2K*$^{-/-}$ mice were more resistant to TNF-α-induced apoptosis (Figure 3G). Moreover, inhibition of protein synthesis by cycloheximide sensitized granulosa cells to TNF-α-induced apoptosis (Figure 3G). Together, these results showed that eEF2K mediates TNF-α-induced apoptosis in granulosa cells and is required for promoting normal follicular atresia.

We further tested whether eEF2K is important for the chemotherapy-induced apoptosis of oocytes. Metaphase II oocytes were collected by superovulation and then treated with 200 nM or 1 μM doxorubicin for 24 hr. *Eef2K*$^{-/-}$ oocytes were more resistant to doxorubicin-induced apoptosis (Figures 3H and 3I) at both doses compared with the response of *Eef2K*$^{+/+}$ oocytes. These results strongly suggest that eEF2K is important for both somatic cell (granulosa cell) death and germ cell (oocyte) death in mice.

Next, we investigated whether inactivation of eEF2K affects the quantity of primordial follicles. While at postnatal day 8 or 2 months of age, the total number of primordial follicles was similar in *Eef2K*$^{-/-}$ mice compared to wild-type (Figures S3C and S3D), the primordial follicle number was ~2-fold higher at 6 months of age and ~3-fold higher at 15 months of age in *Eef2K*$^{-/-}$ mice relative to their wild-type cohorts (Figures S3E and S3F). In addition, 15 month *Eef2K*$^{-/-}$ ovaries had ~2-fold more primary follicles, secondary follicles, and antral follicles compared to wild-type (Figure 3E). To assay the functionality of the preserved primordial follicles, we induced superovulation in 15-month-old female mice by pregnant mare serum gonadotropin (PMSG)/ human chorionic gonadotropin (hCG) and found that oocytes could be retrieved from *Eef2K*$^{-/-}$ mice but not from wild-type mice (Figure 3F). These results showed that inactivation of eEF2K in the mouse did not affect primordial follicle pool until sexual maturation, but displayed a preservation of all types of follicle pools during aging.

We further analyzed female fertility by mating females of various ages with young wild-type males and found that while the litter size of 2- to 6-month-old mothers was unaffected by loss of eEF2K, 8-month-old *Eef2K*$^{-/-}$ mothers produced slightly larger litters than their wild-type cohorts, although this difference

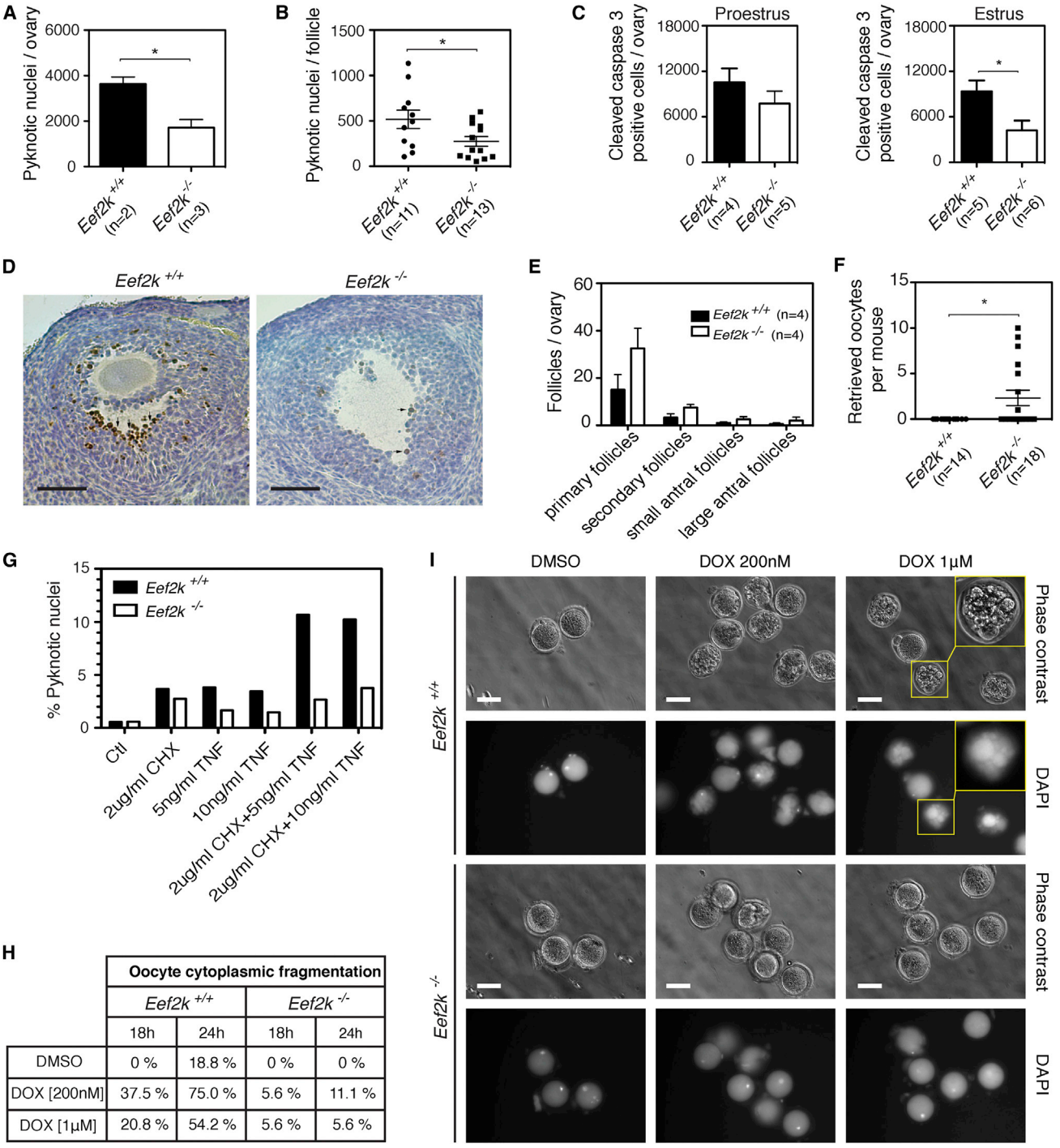

H

	Oocyte cytoplasmic fragmentation			
	Eef2k $^{+/+}$		*Eef2k* $^{-/-}$	
	18h	24h	18h	24h
DMSO	0 %	18.8 %	0 %	0 %
DOX [200nM]	37.5 %	75.0 %	5.6 %	11.1 %
DOX [1μM]	20.8 %	54.2 %	5.6 %	5.6 %

Figure 3. Knockout of eEF2K Reduces Apoptosis Levels in Mouse Ovaries

(A) Quantification of total pyknotic nuclei per ovary in *Eef2K*$^{+/+}$ and *Eef2K*$^{-/-}$ mice. Data are represented as mean ± SEM. *$p < 0.05$ (Mann-Whitney U test).

(B) Quantification of pyknotic nuclei per large atretic follicle with a diameter of over 250 μm in *Eef2K*$^{+/+}$ and *Eef2K*$^{-/-}$ mice. Data are represented as mean ± SEM. *$p < 0.05$ (Mann-Whitney U test).

(C) Quantification of cleaved caspase-3 (CC3) positive granulosa cells per ovary. Data are represented as mean ± SEM. *$p < 0.05$ (Mann-Whitney U test).

(D) Immunohistochemistry of CC3 in follicles of eEF2K$^{+/+}$ and *Eef2K*$^{-/-}$ mice. Scale bars represent 50 μm.

(E) Quantification and analysis of follicles at different developmental stages in *Eef2K*$^{+/+}$ and *Eef2K*$^{-/-}$ ovaries.

(F) Quantification of superovulated oocytes from 15-month-old *Eef2K*$^{+/+}$ and *Eef2K*$^{-/-}$ mice. Data are represented as mean ± SEM. *$p < 0.05$ (Mann-Whitney U test).

(G) Granulosa cells isolated from *Eef2K*$^{+/+}$ and *Eef2K*$^{-/-}$ mice were treated with TNF-α and cycloheximide. Pyknotic nuclei counts were determined by nuclear condensation or chromatin fragmentation with Hoechst 33342 staining. Over 200 nuclei were counted for each experimental group.

(legend continued on next page)

was not statistically significant (p = 0.2244, Figures S3G and S3H). In addition, we found that at 12–16 months of age none of the wild-type mice were pregnant (Figure S3I), but 18% of *Eef2K*$^{-/-}$ females were able to get pregnant. However, these pregnant *Eef2K*$^{-/-}$ females were unable to deliver viable pups due to complications during pregnancy, possibly as a result of the low number of embryos in the uterus and the reabsorption of defective or dead embryos. Thus, knockout of eEF2K did not significantly enhance female fertility and may have increased the risk of fetal death during pregnancy in aged females.

In *C. elegans*, the Phosphorylation of eEF2 Occurs Specifically in the Gonads

eEF2K is highly conserved across eukaryotes, specifically in the N-terminal alpha-kinase catalytic domain and C-terminal eEF2-targeting domain (Figure S6). To test whether the function of eEF2K in germline apoptosis is likewise conserved, we analyzed its role in *C. elegans*, a model system with unique transparency with regards to germ cell development and physiological apoptosis (Kimble and Crittenden, 2007). Consistent with results obtained in the mouse model, the activity of the *C. elegans* homolog of eEF2K, EFK-1, as judged by the level of phosphorylated eEF2 (P-EEF-2), was most intense in the gonads of adult *C. elegans* (Figure 4A). Whole-mount worm immunostaining revealed that the phosphorylation of EEF-2 by EFK-1 was prominent in the distal gonad, from the mitotic distal region that serves to maintain the proliferative germline stem cell pool, through the transition region where germ cell death can occur as cells enter the pachytene stage of meiosis I (Figures 4A and S4A). P-EEF-2 staining could also be observed throughout the proximal gonad where oocytes continue to mature prior to fertilization (Figure 4A).

Loss of eEF2K Reduces Germ Cell Death and Oocyte Quality in *C. elegans*

We next examined physiological germ cell death in the *C. elegans efk-1(ok3609)* mutant that completely lacks EFK-1 kinase activity and exhibits no phosphorylation of EEF-2 (Figure S4B). In *C. elegans*, approximately half of all developing germ cells undergo physiological apoptosis during development in order to maintain germline homeostasis (Gumienny et al., 1999). Using SYTO-12 staining of adult hermaphrodites during peak oocyte production, we found that either genetic knockout or RNAi-mediated knockdown of EFK-1 significantly reduced the number of apoptotic germ cell corpses in the worm gonad (Figures 4B, 4C, S4C, and S4D). Additionally, analysis of *fog-2* mutant worms that are defective for spermatogenesis (Schedl and Kimble, 1988) showed that aged, virgin *efk-1(ok3609); fog-2 (q71)* animals displayed hyperplasia among stacked oocytes in the proximal gonad, which was not observed in *fog-2(q71)* females (Figures S4E and S4F). The germline apoptosis defects of *efk-1* mutants were similar to, albeit milder than those of caspase-defective *ced-3* mutants (Figures 4B, S4E, and S4F), consistent with the idea that eEF2K promotes apoptosis in the *C. elegans* gonad.

It has been proposed that apoptosis is involved in the maintenance of oocyte quality, which can be examined in *C. elegans*, as the size and viability of the laid eggs directly reflects the quality of the oocytes (Andux and Ellis, 2008). We observed that *efk-1(ok3609)* hermaphrodites exhibited an ~5-fold increase in the percentage of small-sized eggs compared to wild-type (Figure 4D). In addition, we also found that *efk-1 (ok3609)* produced ~3-fold more dead embryos than wild-type throughout their reproductive lifespan (Figure 4E). Finally, we examined eggshell integrity and embryo quality by treating gravid hermaphrodites with hypochlorite in order to analyze large pools of synchronized eggs and observed that eggs of older *efk-1(ok3609)* hermaphrodites were twice as likely to die than those of wild-type worms (Figure S4G). Therefore, we concluded that the loss of *efk-1* activity in the *C. elegans* germline results in reduced germ cell apoptosis and oocyte quality.

eEF2K Mediates Protein Synthesis Inhibition and Downregulation of Antiapoptotic Proteins during Apoptosis

To further investigate the mechanism by which eEF2K regulates cell death, we analyzed the levels of phosphorylated eEF2 (p-eEF2) in cultured wild-type cells treated with apoptotic stimuli. Cells cultured under standard conditions did not contain significant quantities of p-eEF2; however, treatment with doxorubicin or H_2O_2 resulted in a dramatic increase in p-eEF2 (Figures 5A and 5B). We then used TUNEL staining to detect apoptosis and found that p-eEF2 was detectable specifically in TUNEL-positive cells (Figure 5C). In fact, nearly all cells that contained apoptotic nuclei, as judged by TUNEL-staining or condensed chromatin, also stained positively for p-eEF2 (Figure S5D). These results suggested that eEF2 phosphorylation by eEF2K in cultured cells was highly associated with programmed cell death.

To investigate the mechanism by which eEF2K affects apoptosis, mouse embryonic fibroblasts (MEFs) isolated from *Eef2K*$^{+/+}$ and *Eef2K*$^{-/-}$ animals were treated with doxorubicin and H_2O_2. Using the MTT assay, we found that *Eef2K*$^{-/-}$ MEFs displayed increased resistance to both agents (Figures S5A and S5B). We analyzed apoptosis in these cells using the TUNEL assay and western blot analysis of cleaved caspase-3 and found that increased resistance in *Eef2K*$^{-/-}$ cells correlated with decreased apoptosis (Figures 5D and 5E). Moreover, the introduction of eEF2K cDNA into *Eef2K*$^{-/-}$ cells sensitized cells to these agents (Figure 5D). These results show that eEF2K is necessary to facilitate oxidative stress-induced apoptosis in murine cells.

Inhibition of protein synthesis is a noted feature of apoptosis (Holcik and Sonenberg, 2005; Piñeiro et al., 2007) but the

(H) Percentage of apoptosis induced by doxorubicin (DOX) in *Eef2K*$^{+/+}$ and *Eef2K*$^{-/-}$ oocytes. Metaphase II oocytes were collected and treated without (DMSO) or with 200 nM or 1 μM doxorubicin. Oocytes with apoptotic morphology (cytoplasmic fragmentation) were quantified. The total number of oocytes analyzed per group was 16–24.

(I) Morphological changes in DOX-treated *Eef2K*$^{+/+}$ and *Eef2K*$^{-/-}$ oocytes. Oocytes were treated with DOX for 24 hr, and then fixed and stained with DAPI. Yellow boxes enlarge the image of an oocyte with cellular fragmentation. Scale bars represent 100 μm.

See also Figures S2 and S3.

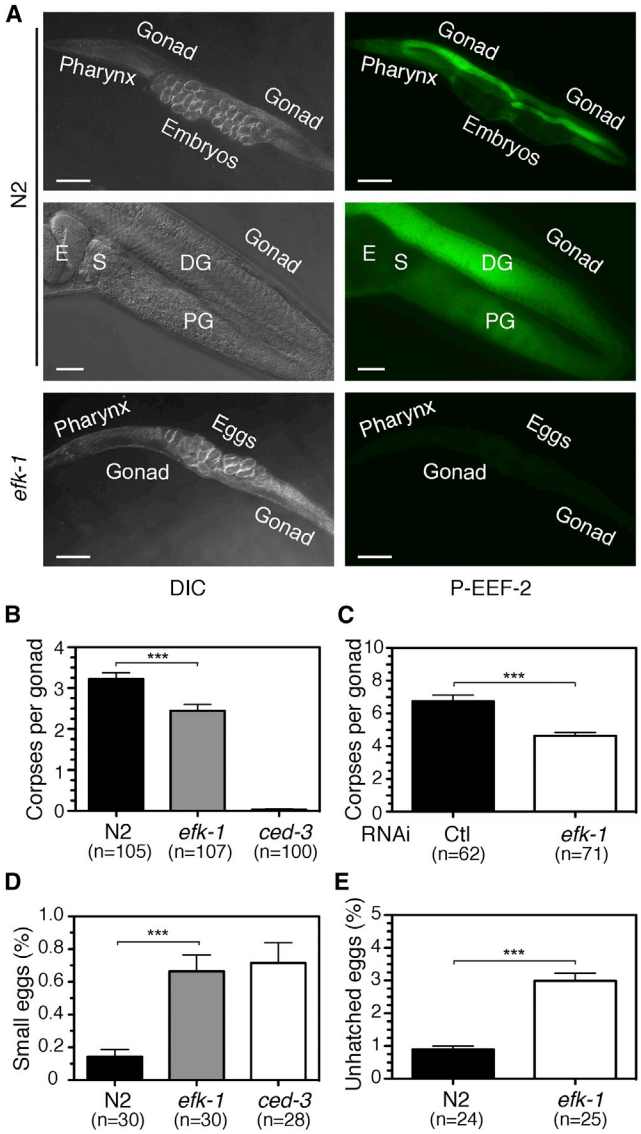

Figure 4. Deficiency of EFK-1, the Homolog of eEF2K in *C. elegans*, Reduces Germ Cell Apoptosis and Oocyte Quality

(A) Whole-mount immunostaining of phosphorylated EEF-2 by EFK-1 in the gonads of N2 and *efk-1(ok3609)* adult *C. elegans*. Scale bars represent 100 μm (top and bottom panels) and 20 μm (middle panel). DG, distal gonad; PG, proximal gonad; E, embryo; S, spermatheca.

(B) Quantification of germ cell corpses per gonad in the N2, *efk-1(ok3609)*, and *ced-3(n717)* by SYTO-12 staining. Data are represented as mean ± SEM. ***p < 0.001 (Mann-Whitney U test).

(C) Quantification of germ cell corpses per gonad by SYTO-12 staining after RNAi (control or *efk-1*) in the *ced-1(e1754)* mutant that retains corpses due to a defect in cell engulfment. Data are represented as mean ± SEM. ***p < 0.001 (Mann-Whitney U test).

(D) Percentage of small-sized eggs produced during reproductive lifespan in N2, *efk-1(ok3609)*, and *ced-3(n717)*. Data are represented as mean ± SEM. ***p < 0.001 (Mann-Whitney U test).

(E) Percentage of unhatched eggs produced during reproductive lifespan in N2 and *efk-1(ok3609)*. Data are represented as mean ± SEM. ***p < 0.001 (Mann-Whitney U test).

See also Figures S4 and S6.

mechanisms of this inhibition have remained unclear. To investigate whether phosphorylation of eEF2 by eEF2K contributes to this inhibition, we compared the rate of protein synthesis in MEFs with and without eEF2K following treatment with doxorubicin. We found that by 9–12 hr after treatment, doxorubicin caused a significant decrease in protein synthesis in cells expressing eEF2K but not in eEF2K-deficient cells (Figures 5F and S5E). This inhibition of protein synthesis occurred within the time frame where the highest levels of eEF2 phosphorylation were observed (Figure 5G). Thus, our results suggest that the inhibition of global protein synthesis during apoptosis is mediated, in part, by the phosphorylation of eEF2.

It has been suggested that inhibition of protein synthesis may promote apoptosis by selectively decreasing levels of short-lived antiapoptotic proteins, such as c-FLIP$_L$ and XIAP (Fulda et al., 2000; Holley et al., 2002; White et al., 2007). To test whether eEF2K activity affected these antiapoptotic proteins, we measured their levels during apoptosis. In cells expressing eEF2K, we observed a progressive decrease in c-FLIP$_L$ and XIAP levels that correlated with the activation of eEF2K after doxorubicin treatment (Figure 5G); however, in eEF2K-deficient cells there was no significant decline in the amount of these proteins (Figure 5G). Moreover, knockdown of eEF2 by siRNA in MEFs mimicked eEF2K function and lowered c-FLIP$_L$ and XIAP protein expression (Figure 5H). To test whether the downregulation of c-FLIP$_L$ and XIAP is due to the activation of caspase, we inactivated caspase activity by adding the broad-spectrum caspase inhibitor, QVD-OPh, prior to doxorubicin treatment. Western blot analysis showed that levels of c-FLIP$_L$ and XIAP were not restored in QVD-OPh pretreated cells (Figure S5C), indicating that caspase activity was dispensable for the downregulation of c-FLIP$_L$ and XIAP. This suggests that eEF2K activity promotes apoptosis, at least in part by mediating a decrease in levels of antiapoptotic proteins c-FLIP$_L$ and XIAP.

DISCUSSION

The results presented here suggest that eEF2K functions to maintain germline quality by regulating programmed germ cell death. We report that ovaries derived from eEF2K knockout mice exhibit reduced granulosa cell death and abnormal antral follicles that failed to be degenerated; while similar phenotypes have been reported in mice with a null mutation of caspase-3 or an overexpression of bcl-2 (Matikainen et al., 2001; Morita et al., 1999). This would suggest that eEF2K may play a role in the cell death pathway during ovarian cell death and provide a link between the regulation of protein synthesis and apoptosis. Although we observed that knockout of eEF2K preserved the follicle pool at advanced reproductive age, the oocytes of those follicles were unhealthy and unable to form progeny. Similarly, we demonstrated that the loss of *efk-1* in *C. elegans* resulted in a decline in oocyte quality and embryo survival, as well as a reduction in germ cell death, a phenotype similar to the knockout of the caspase homolog *ced-3* in this organism. Our results suggest a mechanism by which the inhibition of protein synthesis by eEF2K regulates apoptosis in the germline and acts as a means of selection of the highest quality, most robust oocytes that will go on to ovulate and form progeny.

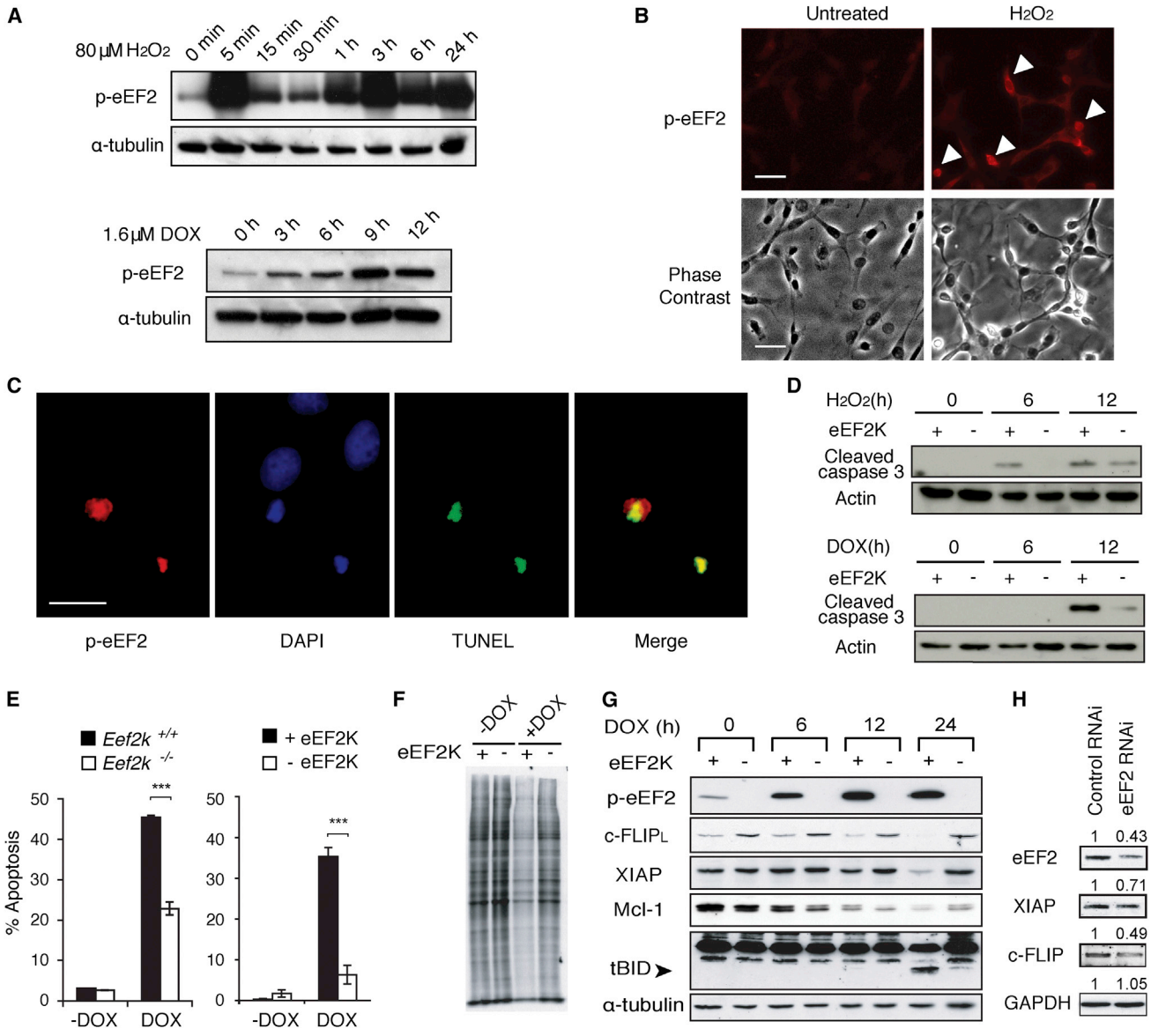

Figure 5. eEF2K Is Activated during Apoptosis and Regulates It through Downregulation of Short-Lived Antiapoptotic Proteins

(A) Western blot analysis of p-eEF2 levels in H_2O_2-treated NIH 3T3 cells or doxorubicin (DOX)-treated MEFs.

(B) Immunostaining of p-eEF2 in NIH 3T3 cells exposed to 400 μM H_2O_2 for 3 hr compared to untreated cells. Scale bars represent 20 μm.

(C) Immunofluorescent staining in HeLa cells treated with 1 μM doxorubicin for 18 hr; p-eEF2, DAPI, and TUNEL staining are shown. Scale bars represent 10 μm.

(D) Analyzed of cleaved caspase-3 levels by western blot in H_2O_2 and doxorubicin-treated knockout MEFs expressing vector alone (−eEF2K) or vector containing eEF2K cDNA (+eEF2K).

(E) Apoptosis analyzed by TUNEL assay in H_2O_2 and doxorubicin-treated wild-type (*Eef2K*$^{+/+}$), knockout (*Eef2K*$^{-/-}$), and knockout MEFs expressing vector alone (−eEF2K) or vector containing eEF2K cDNA (+eEF2K). Data are represented as mean ± SEM. ***$p < 0.002$ (two-tailed t test).

(F) Measurement of protein synthesis in knockout MEFs expressing vector alone (−eEF2K) or vector containing eEF2K cDNA (+eEF2K) treated with doxorubicin for 12 hr and labeled with ^{35}S-methionine.

(G) Western blot analysis of p-eEF2, c-FLIP$_L$, XIAP, Mcl-1, tBID, and α-tubulin in doxorubicin-treated MEFs expressing vector alone (−eEF2K) or vector containing eEF2K cDNA (+eEF2K).

(H) Western blot analysis of eEF2, XIAP, c-FLIP$_L$, and GAPDH in eEF2 knockdown MEFs.

See also Figure S5.

Genetic mutations in mice reveal that apoptosis in oocytes is involved in the control of oocyte numbers (Pru and Tilly, 2001); however, the increase of oocyte numbers may not positively correlate with a gain of function in fertility. For example, BAX null female mice show preserved primordial follicles at advanced reproductive age, but are unable to become pregnant despite this fact (Perez et al., 1999). In addition, the genetic ablation of caspase-2 in mice displayed an increase in primordial follicles, but also did not affect female fertility (Bergeron et al., 1998). *Eef2K*$^{-/-}$ mice display an increase in the numbers of all types

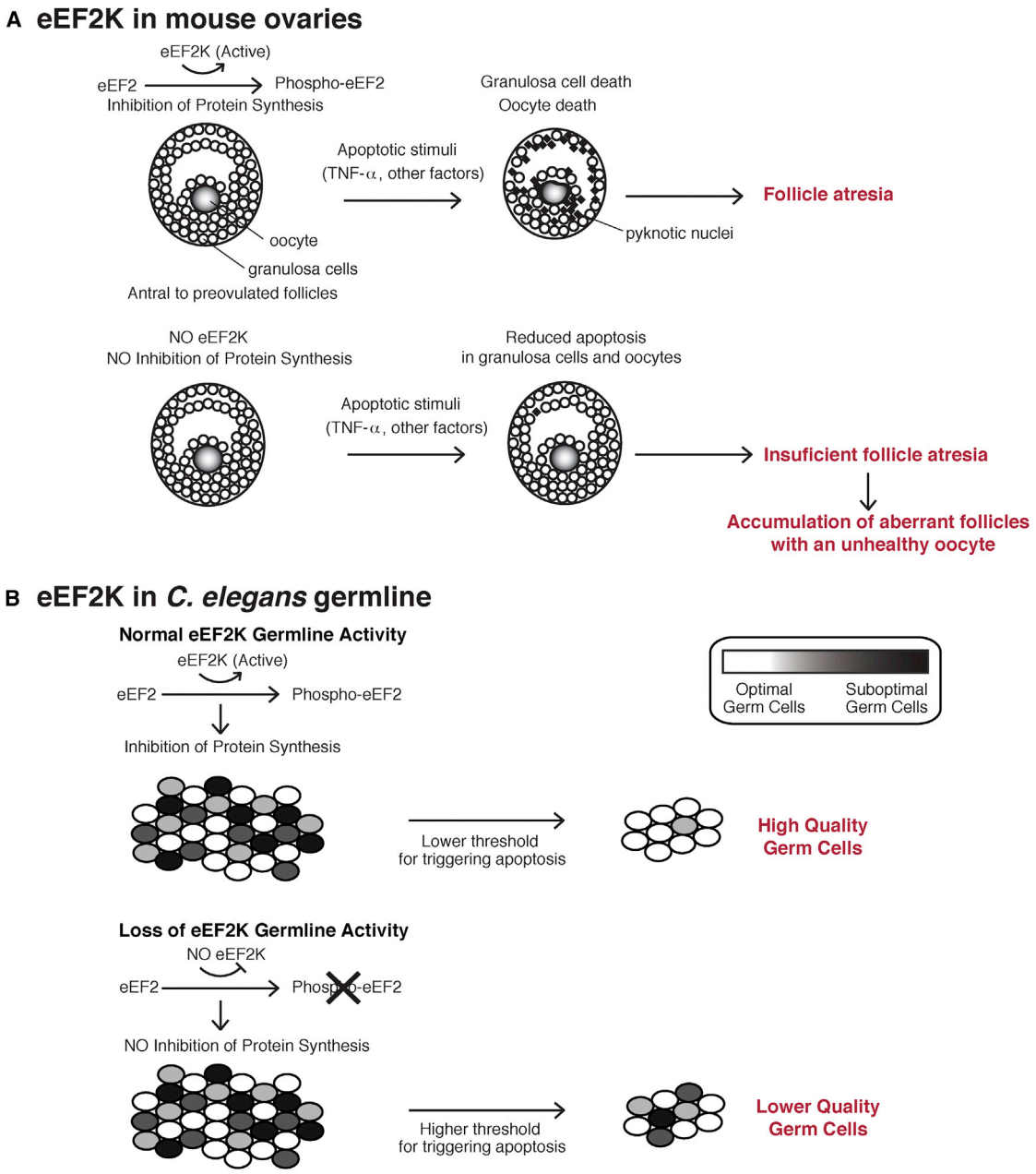

Figure 6. Germline Maintenance by eEF2K

(A) Model of ovarian cell death in mouse ovaries. In this model, inhibition of protein synthesis by eEF2K sensitizes granulosa cells and oocytes to apoptotic stimuli and promotes follicle atresia. Insufficient follicle atresia in *Eef2K*$^{-/-}$ ovaries results in the accumulation of aberrant follicles with unhealthy oocytes.

(B) Model of germ cell death in *C. elegans*. In this model, eEF2K regulates protein synthesis thereby adjusting the threshold for apoptosis during germline development and selection. The high activity of eEF2K results in a more restrictive cellular environment, which increases selective pressure and lowers the threshold for triggering apoptosis in order to produce high quality germ cells.

of ovarian follicle at advanced age, but similarly do not show a significant increase in female fertility. These results suggest that female fertility in mammals is regulated by multiple factors, such as the number of healthy, mature follicles and the regulation of hormones.

Our studies suggest that the defects occurring in the absence of eEF2K are due to defects in granulosa cell death, oocyte death, and follicle atresia (Figures 3A–D and 3G–3I). We observed many abnormal follicles containing an unhealthy oocyte that displayed no sign of granulosa cell death (Figure 2C). These results therefore suggest that granulosa cell death is required for follicle degeneration and that defects in granulosa cell death may result in the accumulation of defective oocytes in ovaries (Figure 6A). In addition, we have shown here that eEF2K sensitizes TNF-α-induced apoptosis in granulosa cell death, which suggests that combination of eEF2K-mediated

protein synthesis inhibition with TNF-α signaling could be the mechanism that regulates follicle atresia. Moreover, the decrease in oocyte quality is accompanied by an increase in DNA damage (Titus et al., 2013) and oxidative damage (Lim and Luderer, 2011) with age. Because knockout of eEF2K in MEFs or oocytes prevents apoptosis from genotoxic and oxidative stress, this suggests that an accumulation of unhealthy oocytes at advanced age in *Eef2K*$^{-/-}$ ovaries could also be due to a defect of apoptosis in oocytes (Figure 6A). The observed accumulation of unhealthy oocytes in *Eef2K*$^{-/-}$ mice is consistent with the hypothesis that lack of eEF2K affects elimination of poor quality in *C. elegans*. Although the evidence suggesting that poor quality (unhealthy) oocytes are moved forward in developmental process because of defects in apoptosis is stronger in *C. elegans* than in mice, the defects of ovarian apoptosis in *Eef2K*$^{-/-}$ mice positively correlates with an accumulation of unhealthy oocytes.

Apoptosis is usually accompanied by an inhibition of global protein synthesis. Our results show that intense phosphorylation of eEF2 is highly associated with apoptotic cells, suggesting that translational arrest achieved by phosphorylation of eEF2 could contribute to the inhibition of protein synthesis during apoptosis. Indeed, we observed that eEF2K activity led to a substantial suppression in protein synthesis during apoptosis induced by doxorubicin, while only a slight decrease was observed in eEF2K knockout cells. It is still not clear how inhibition of protein synthesis affects apoptosis. Apoptosis is controlled by the relative concentration and activity of various pro- and antiapoptotic proteins. Although most proapoptotic proteins have relatively long half-lives, many antiapoptotic proteins such as c-FLIP$_L$ and XIAP are short-lived. Such short-lived proteins are continually degraded and need to be constantly resynthesized to maintain their levels. Consequently, inhibition of protein synthesis can lead to a rapid decline in intracellular levels of antiapoptotic proteins. As suggested by previous studies, the inhibition of protein translation may play an important role in apoptosis by modulating the level of short-lived antiapoptotic proteins (Adams and Cooper, 2007; Fulda et al., 2000; Holley et al., 2002). Thus, our study supports this hypothesis, demonstrating that inhibition of protein synthesis by eEF2K leads to the downregulation of these short-lived antiapoptotic proteins.

Despite the fact that females are born with millions of oocytes, only a few hundred of them successfully reach maturity and ovulate during their lifetime. The loss of oocytes is driven by ovarian cell death and has been hypothesized to contribute to the selective elimination of unhealthy oocytes. A recent theory suggests that this selection is based on filtering out oocytes containing severely mutated mtDNA genomes (Fan et al., 2008; Stewart et al., 2008). In addition, mtDNA undergoes a drastic increase in copy number during oocyte maturation (Cao et al., 2007), suggesting that clonal expansion and selection may occur. Mammalian mtDNA has a relatively high mutation rate and is only inherited maternally. Evidence has shown that mitochondrial DNA mutations lead to increased oxidative stress and that oocytes carrying severely compromised mitochondria could be eliminated after only a few generations (Fan et al., 2008). As this study demonstrates, oxidative stress induces intense phosphorylation of eEF2 and cells derived from *Eef2K*$^{-/-}$ mice are more tolerant to oxidative stress than wild-type cells, thereby suggesting that eEF2K may play a role in facilitating apoptosis in the ovary to eliminate defective oocytes with mitochondrial mutations that generate oxidative stress.

The mechanism by which germ cell selection is accomplished during oogenesis remains obscure. One possibility could be related to cell competition, which is a process required to eliminate suboptimal cells in order to maintain the fitness of a cell population or tissue (Johnston, 2009; Levayer and Moreno, 2013). Cell competition was first described in *Drosophila* where mutations, termed "*Minutes*," in genes encoding ribosomal proteins led to impaired cell competition and cell fitness during embryonic development (Lambertsson, 1998). Here, we show that eEF2K knockout in mice impairs ovarian homeostasis and results in the accumulation of aberrant follicles in aged mice, implying a link between the regulation of protein synthesis and the maintenance of oocyte quality. In addition, it has also been reported that the rate of protein synthesis is a critical parameter affecting cell competition, positively correlating with the "winner" cell population (Clavería et al., 2013). Our study suggests that activation of eEF2K and the phosphorylation of eEF2 facilitate a selective, apoptosis-driven process to eliminate suboptimal germ cells. We propose a model where eEF2K-mediated inhibition of global protein synthesis lowers the threshold for triggering apoptosis (Figure 6B) in order to maintain germline quality. Our data suggest that phosphorylation of eEF2 by eEF2K may be a general mechanism in metazoans whereby suppression of protein synthesis helps reveal defective cells and maintain the fitness of a population.

EXPERIMENTAL PROCEDURES

Immunohistochemistry

Tissues were fixed in 4% paraformaldehyde and embedded in paraffin. Tissues were serially sectioned (4 μm), mounted on glass slides, and subjected to immunohistochemical staining for the presence and distribution of p-eEF2 (Cell Signaling, catalog #2331) and cleaved caspase-3 (R&D Systems, catalog #AF835). Antigen unmasking was performed in 10 mM sodium citrate pH 6.0 with 0.1% Tween 20. Sections were then washed and blocked with tris- buffered saline Tween20 (TBST) buffer (100 mM Tris-HCl [pH 7.5], 9% NaCl, 0.025% Triton X-100) supplemented with 1% BSA and 10% normal goat serum and then incubated with primary antibody diluted 1:200 in 1% BSA in tris-buffered saline (TBS). The secondary antibody was prepared from biotinylated antibody stock of Vectastain Elite ABC Kit (Vector Labs). After incubation, sections were incubated in 3% hydrogen peroxide, followed by Vectastain Elite ABC and finally ImmPACT DAB peroxidase substrate (Vector Labs). Sections were counterstained with hematoxylin. For immunofluorescence staining, tissue were serially sectioned (4 μm), mounted on glass slides, and subjected to immunofluorescent staining for the presence and distribution of p-eEF2. Procedures were similar to DAB reaction through incubation of primary antibody. Sections were then incubated in Alexa Fluor secondary antibody (Molecular Probes). Finally, sections were incubated in DAPI (5 μg/ml in TBS). Sections were mounted with ProLong antifade reagent (Molecular Probes). For HeLa cell immunostaining, 1:100 dilution of p-eEF2 antibody was used. Staining was performed according to the manufacturer's instructions (Cell Signaling).

Construction of *Eef2K*$^{-/-}$ Mice

The mouse *Eef2K* gene was cloned from a 129 SV phage genomic library. The targeting vector was constructed by using a 1.2 kb DNA fragment as the short arm, which was a PCR fragment from the end of exon 8 to exon 10 (primer pairs: SA2 with a sequence of 5′-TGGAGATGGTAACCTTG-3′, SA4 with a sequence of 5′-TCAAGATGGTCTTGG CTGATTG-3′). The long arm was the BamHI fragment, which contains exon 6. In this knockout strategy, the entire

exon 7 and majority of exon 8 have been replaced by the neo gene cassette. After electroporation of embryonic stem cells, surviving colonies in G418 were expanded, and PCR analysis was performed to identify clones that had undergone homologous recombination. PCR was done using primer pairs SA8 (5′-GGCCGGCTGCTAGAGAGTGTC-3′) and Neo1 (5′-TGCGAGGCCA GAGGCCACTTGTGTAGC-3′). The correctly targeted ES cell lines were microinjected into C57BL/6J host blastocysts. The chimeric mice were generated and they gave germline transmission of the disrupted *Eef2K* gene. The genotyping of *Eef2K*$^{-/-}$ mice was performed using PCR with two pairs of primers (Neo1/SA8, SA8/SA5, sequence of SA5: 5′-CATCAGCTGATTGTAGTGGA CATC-3′). To create a congenic strain, heterozygous mice were backcrossed to the C57BL/6 strain for ten generations, then heterozygous mice were intercrossed to obtain wild-type and knockout mice. The Institutional Animal Care and Use Committee at the Rutgers University-Robert Wood Johnson Medical School approved the animal and surgical procedures performed in this study.

Preparation of MEFs

MEFs were prepared from E13.5 embryos. Immortalized cell lines were obtained via retrovirus infection with SV40 large T antigen. The virus particles were collected from the medium of transiently triple-transfected 293T cells by three plasmids including VSV, gal/pol, and pBebe-neo. For introduction of the *Eef2K* gene into *Eef2K*$^{-/-}$ MEFs, the pLXSP retrovirus vector carrying mouse eEF2K cDNA was cotransfected with VSV and gal/pol plasmids to produce virus particles. After viral infection, infected cells were selected in puromycin-containing medium.

TUNEL Assay

For TUNEL assay, cells were collected and fixed in 1% paraformaldehyde for 15 min on ice. Cells were stored in 75% ethanol at –20°C until staining, which was performed according to the manufacturer's instructions (In Situ Cell Death Detection kit, Roche Diagnostics). Apoptotic cells were labeled with fluorescein and analyzed by flow cytometry.

eEF2 RNA Interference

Small interfering RNA (siRNA) oligonucleotides specifically targeting the 5′UTR of mouse eEF2 were designed using the IDT online design tool and synthesized by IDT. MEFs at a density of ~30% were transfected with siRNA using N-TER transfection reagent (Sigma) with a serum-free medium following the manufacturer's recommendations. Nonspecific siRNA was purchased from Invitrogen; mouse eEF2 siRNA was designed to target the 5′UTR of eEF2 (sequence: TCCCTGTTCACCTCTGACT).

Western Blot

Antibodies against eEF2, phosphorylated eEF2, cleaved caspase3 (5A1), XIAP (Cell Signaling), mouse eEF2K (BD Biosciences), mouse c-FLIP$_L$ (Dave-2) (Alexis Biochemicals), mouse Mcl-1 (Rockland) BID (AF860) (R&D System), actin (AC-40), and α-tubulin (B-5-1-2) (Sigma) were used. For western blotting, cells were lysed in SDS lysis buffer (20 mM HEPES in pH 7.5, 50 mM NaCl, 25 mM KCl, 10 mM DTT, 3 mM benzamidine, 1% SDS, 1 mM sodium orthovanadate, 20 mM sodium pyrophosphate, 1 tablet of complete protease inhibitor [Roche Diagnostics] per 10 ml buffer) to block phosphorylation reaction in vitro. For *C. elegans*, western blot lysates were prepared by collecting adult *C. elegans* in RIPA buffer (15 mM HEPES, 150 mM NaCl, 3 mM $MgCl_2$, 1 mM EDTA, 5% sodium deoxycholate, 0.01% NP-40, 2% SDS, 1 tablet complete protease inhibitor [Roche Diagnostics] per 10 ml buffer). Western blotting was performed according to the manufacturer's instructions (Cell Signaling).

Pyknotic Nuclei Counts

Ovaries were serially sectioned (8 μm) and stained with hematoxylin. Every other section was analyzed for the presence of pyknotic nuclei. Atretic follicles were identified by the presence of pyknotic nuclei in more than 1% of granulosa cells. Total pyknotic nuclei in granulosa cells per ovary were counted. Antral follicles over 250 μm in diameter were analyzed to determine pyknotic nuclei density per follicle.

Cleaved Caspase-3 Quantification in Ovaries

Ovaries at proestrus and estrus phases of estrous cycle were dissected from mice analyzed by vaginal smears, fixed in 10% neutral-buffered formalin solution, and embedded in paraffin. Serially sectioned (5 μm) ovary tissues were placed in order on glass microscope slides and immunostained with cleaved caspase-3 antibodies (1:500, Cell Signaling). Apoptotic cells were identified as brown stained cells. The number of apoptotic granulosa cells was counted in every tenth section. The total number of apoptotic cells was calculated by multiplying cumulative counts by a factor of 10. To statistically compare the difference between *Eef2K*$^{+/+}$ and *Eef2K*$^{-/-}$ mice, Mann-Whitney U test was applied.

Superovulation and 15-Month-Old Follicle Counts

To retrieve oocytes from 15-month-old female mice, 7.5 IU PMSG (Sigma) was subcutaneously injected to stimulate follicle growth. A single subcutaneous injection of 7.5 IU hCG (Sigma) was followed 48 hr later. Ovulated oocytes were collected from the ampullae of the oviducts 16 hr after hCG injection. Ovaries were collected after superovulation, fixed, embedded in paraffin, and serially sectioned (8 μM). Serial sections were also stained with picric methyl blue and follicles at different developmental stages were counted in every tenth section. The overall number of follicles was calculated by multiplying counts by a factor of 10.

In Vitro Granulosa Cell Cultures

Young wild-type and eEF2K-deficient female mice (~4 weeks of age) were injected with 10 IU PMSG (Calbiochem), and ovaries were dissected after 42 hr. The stimulated follicles were punctured with a 25 gauge needle to collect granulosa cells into Waymouth's MB752/1 medium (Life Technology) supplemented with 20% FBS (Life Technology), 1× PSG, 1× ITS, and 1 mM sodium pyruvate. Granulosa cells were cultured for 24 hr, until cells reached confluence. Afterward, cells were treated with the indicated concentrations of TNF-α and cycloheximide for 24 hr. Cells were then fixed in methanol:acetic acid (3:1) for 15 min at 4°C and stained with 10 μg/ml Hoechst 33342 at 37°C for 20 min.

Oocyte Collection and Culture

Female mice (3–4 months old) were superovulated with 10 IU PMSG (Calbiochem), followed 46 hr later by injection with 7.5 IU hCG (Calbiochem). Mature oocytes were collected 16 hr following hCG injection. Cumulus cells were removed by brief incubation in 80 IU hyaluronidase (Sigma). Oocytes were cultured throughout the experiment in 0.2 ml of human tubal fluid (Irvine Scientific) supplemented with 0.5% BSA (Sigma) under mineral oil at 37°C and 5% CO_2. Oocytes were treated with 200 nM or 1 μM doxorubicin (DOX) (Sigma) or DMSO (Control) for 24 hr and analyzed for cytoplasmic fragmentation every 2 hr. Following treatment, oocytes were stained with DAPI and further inspected. The *Eef2K*$^{+/+}$ oocyte sample size was 16–24 oocytes per treatment group, and the *Eef2K*$^{-/-}$ oocyte population size was 18–19 oocytes per treatment group.

Primordial Follicle Counts

To evaluate the total number of primordial follicles, three or more mice of different genotypes were sacrificed at various ages. Ovaries were fixed (0.34 N glacial acetic acid, 10% formalin, and 28% ethanol), embedded in paraffin, and serially sectioned (8 μm). The serial sections were stained with picric methyl blue and the number of primordial follicles was counted in every fifth section. To obtain the total number of primordial follicles, the cumulative follicle counts were multiplied by a factor of 5 representing the total number of sections.

Measurement of Protein Synthesis with ^{35}S Labeling

For ^{35}S labeling, 3 × 10^5 cells/well were grown in 6 cm plates overnight. Cells were treated with 1.6 μM doxorubicin for 12 hr. After 12 hr, media was changed to Met, Cys-free RPMI1640 (with 10% dialyzed FBS and 1.6 μM doxorubicin) for 60 min. [^{35}S] methionine/cysteine (100 μCi) was added into RPMI1640 medium for 1 hr and then cells were lysed in M-PER Mammalian Protein Extraction Reagent (Pierce). ^{35}S-labeled proteins were visualized by autoradiography after electrophoresis.

C. elegans Strains and Growth Conditions

C. elegans strains were cultured on NGM plates seeded with *Escherichia coli* strain OP50 at 20°C according to standard procedures as described (Brenner,

1974). The N2 Bristol strain was used as the reference wild-type strain in this study. The *C. elegans* alleles used in this study include: *efk-1(ok3609)*, *ced-3 (n717)* (Yuan et al., 1993), *ced-1(e1754)* (Hedgecock et al., 1983), *fog-2(q71)* (Schedl and Kimble, 1988), *efk-1(ok3609);fog-2(q71)*, and *ced-3(n718); fog-2(q71)*. The *efk-1(ok3609)* strain was constructed by the *C. elegans* Gene Knockout Project, which is part of the International *C. elegans* Gene Knockout Consortium.

C. elegans Immunostaining

C. elegans whole-mount immunostaining was performed as previously described (Finney and Ruvkun, 1990). Samples were probed with primary antibodies against phospho-eEF2 (Thr56) (Cell Signaling) and used at a 1:150 dilution. Secondary antibodies conjugated to Alexa Fluor 488 dye (Molecular Probes) were used at a 1:1,000 dilution. Images were acquired on a Zeiss Axioskop 2 Plus microscope.

C. elegans Embryonic Lethality Assay

C. elegans hermaphrodites were transferred to fresh plates every 24 hr once fully matured in order to quantify the number of egg and unhatched dead eggs produced during the hermaphrodite reproductive span. The proportion of eggs that failed to hatch was determined. In addition, synchronized hermaphrodite *C. elegans* were subjected to 0.5% hypochlorite treatment at various stages of adult reproductive development in order to dissolve hermaphrodites and obtain large quantities of fertilized eggs. The proportion of eggs that failed to hatch was determined 24 hr posttreatment.

C. elegans Germ Cell Corpse Assays

C. elegans hermaphrodites were stained with SYTO 12 (Molecular Probes). Animals were stained as previously described (Gumienny et al., 1999) in 33 μM SYTO-12 solution for 4 hr at 23°C. Animals were anesthetized in 2 mM levamisole, mounted on agarose pads, and stained corpses were identified. Additionally, germ cell corpses were analyzed in the *ced-1(e1754)* mutant. We used RNA interference (RNAi) obtained from the *C. elegans* RNAi v1.1 feeding library (Open Biosystems). RNAi feeding was performed as previously described (Timmons and Fire, 1998). *E. coli* (HT115)-producing double-stranded RNA (dsRNA) for *efk-1* gene were seeded onto NGM plates containing 50 μg/ml carbenicillin and 5 mM IPTG to induce dsRNA expression. The negative RNAi control (HT115) containing empty vector pL4440 was used. Animals were grown on RNAi bacterial plates for two generations and corpses were scored in adults animals aged 24 hr from the onset of ovulation.

C. elegans Oocyte Quality Analysis

Oocyte quality was analyzed through the quantification of small eggs produced during the reproductive lifespan of hermaphrodite *C. elegans*. Eggs were classified as small if they were <75% of normal size. Eggs <25% of normal size were excluded from the small classification and considered unviable. Additionally, the gonads of aged *fog-2(q71)* animals were analyzed as they lack spermatogenesis creating female XX animals and normal XO animals (Schedl and Kimble, 1988). Animals were aged 72 hr at 20°C following the L4-molt. The proximal gonad containing stacked, unfertilized oocytes was observed for hyperplasia and the number of oocytes per proximal gonad. In wild-type, stacked oocytes occupy the entire cross-sectional slice of the gonad; hyperplasia was identified when smaller oocytes were found stacked on top of one another within a given slice of the gonad.

SUPPLEMENTAL INFORMATION

Supplemental Information includes Supplemental Experimental Procedures and six figures and can be found with this article online at http://dx.doi.org/10.1016/j.devcel.2014.01.027.

AUTHOR CONTRIBUTIONS

This study was designed by H.-P.C., Y.L., J.S.N., R.E.E., and A.G.R. Mouse experiments were performed and analyzed by H.-P.C., Y.L., J.S.N., Z.H., J.J.M., Y.S., M.V.D., A.N., P.M.C., R.G.N., and D.E.H. *C. elegans* experiments were performed and analyzed by J.S.N., B.P.B, and R.E.E. Manuscript was written and prepared by H.P.C., Y.L., J.S.N., and A.G.R.

ACKNOWLEDGMENTS

We are grateful to E. Shor for many helpful suggestions on the manuscript. We would like to thank E. White for her discussions on the TNF-α-induced apoptosis pathway, J.L. Tilly and H.J. Lee for their expertise regarding in vitro culture of granulosa cells, and K. Schindler for reagents and her expertise regarding in vitro culture of oocytes. Some *C. elegans* strains were provided by the Caenorhabditis Genetics Center (CGC), which is funded by the National Institutes of Health (NIH) Office of Research Infrastructure Programs (P40 OD010440); other strains were graciously provided by M.C. Soto. We would like to thank C. Rongo and A. Singson for providing access to their *C. elegans* RNAi libraries and B.D. Grant for technical expertise regarding *C. elegans* immunostaining. This work was supported by NIH grants: R01GM57300, R01CA81102, R01AG19890, RC1AI078513, R03TW008217, R21AG042870 (A.G.R.), and R01 GM085282 (R.E.E.). A.G.R. is the founder of Longevica Pharmaceuticals, a company involved in the development of eEF2K inhibitors.

Received: September 13, 2013
Revised: December 11, 2013
Accepted: January 27, 2014
Published: February 27, 2014

REFERENCES

Adams, K.W., and Cooper, G.M. (2007). Rapid turnover of mcl-1 couples translation to cell survival and apoptosis. J. Biol. Chem. *282*, 6192–6200.

Andux, S., and Ellis, R.E. (2008). Apoptosis maintains oocyte quality in aging Caenorhabditis elegans females. PLoS Genet. *4*, e1000295.

Bergeron, L., Perez, G.I., Macdonald, G., Shi, L., Sun, Y., Jurisicova, A., Varmuza, S., Latham, K.E., Flaws, J.A., Salter, J.C., et al. (1998). Defects in regulation of apoptosis in caspase-2-deficient mice. Genes Dev. *12*, 1304–1314.

Brenner, S. (1974). The genetics of Caenorhabditis elegans. Genetics *77*, 71–94.

Browne, G.J., and Proud, C.G. (2002). Regulation of peptide-chain elongation in mammalian cells. Eur. J. Biochem. *269*, 5360–5368.

Cao, L., Shitara, H., Horii, T., Nagao, Y., Imai, H., Abe, K., Hara, T., Hayashi, J., and Yonekawa, H. (2007). The mitochondrial bottleneck occurs without reduction of mtDNA content in female mouse germ cells. Nat. Genet. *39*, 386–390.

Clavería, C., Giovinazzo, G., Sierra, R., and Torres, M. (2013). Myc-driven endogenous cell competition in the early mammalian embryo. Nature *500*, 39–44.

Fan, W., Waymire, K.G., Narula, N., Li, P., Rocher, C., Coskun, P.E., Vannan, M.A., Narula, J., Macgregor, G.R., and Wallace, D.C. (2008). A mouse model of mitochondrial disease reveals germline selection against severe mtDNA mutations. Science *319*, 958–962.

Finney, M., and Ruvkun, G. (1990). The unc-86 gene product couples cell lineage and cell identity in C. elegans. Cell *63*, 895–905.

Fulda, S., Meyer, E., and Debatin, K.M. (2000). Metabolic inhibitors sensitize for CD95 (APO-1/Fas)-induced apoptosis by down-regulating Fas-associated death domain-like interleukin 1-converting enzyme inhibitory protein expression. Cancer Res. *60*, 3947–3956.

Gumienny, T.L., Lambie, E., Hartwieg, E., Horvitz, H.R., and Hengartner, M.O. (1999). Genetic control of programmed cell death in the Caenorhabditis elegans hermaphrodite germline. Development *126*, 1011–1022.

Hedgecock, E.M., Sulston, J.E., and Thomson, J.N. (1983). Mutations affecting programmed cell deaths in the nematode Caenorhabditis elegans. Science *220*, 1277–1279.

Holcik, M., and Sonenberg, N. (2005). Translational control in stress and apoptosis. Nat. Rev. Mol. Cell Biol. *6*, 318–327.

Holley, C.L., Olson, M.R., Colón-Ramos, D.A., and Kornbluth, S. (2002). Reaper eliminates IAP proteins through stimulated IAP degradation and generalized translational inhibition. Nat. Cell Biol. *4*, 439–444.

Johnston, L.A. (2009). Competitive interactions between cells: death, growth, and geography. Science *324*, 1679–1682.

Kimble, J., and Crittenden, S.L. (2007). Controls of germline stem cells, entry into meiosis, and the sperm/oocyte decision in Caenorhabditis elegans. Annu. Rev. Cell Dev. Biol. *23*, 405–433.

Kreuz, S., Siegmund, D., Scheurich, P., and Wajant, H. (2001). NF-kappaB inducers upregulate cFLIP, a cycloheximide-sensitive inhibitor of death receptor signaling. Mol. Cell. Biol. *21*, 3964–3973.

Lambertsson, A. (1998). The minute genes in Drosophila and their molecular functions. Adv. Genet. *38*, 69–134.

Leprivier, G., Remke, M., Rotblat, B., Dubuc, A., Mateo, A.R., Kool, M., Agnihotri, S., El-Naggar, A., Yu, B., Somasekharan, S.P., et al. (2013). The eEF2 kinase confers resistance to nutrient deprivation by blocking translation elongation. Cell *153*, 1064–1079.

Levayer, R., and Moreno, E. (2013). Mechanisms of cell competition: themes and variations. J. Cell Biol. *200*, 689–698.

Lim, J., and Luderer, U. (2011). Oxidative damage increases and antioxidant gene expression decreases with aging in the mouse ovary. Biol. Reprod. *84*, 775–782.

Matikainen, T., Perez, G.I., Zheng, T.S., Kluzak, T.R., Rueda, B.R., Flavell, R.A., and Tilly, J.L. (2001). Caspase-3 gene knockout defines cell lineage specificity for programmed cell death signaling in the ovary. Endocrinology *142*, 2468–2480.

Micheau, O., Lens, S., Gaide, O., Alevizopoulos, K., and Tschopp, J. (2001). NF-kappaB signals induce the expression of c-FLIP. Mol. Cell. Biol. *21*, 5299–5305.

Morita, Y., Perez, G.I., Maravei, D.V., Tilly, K.I., and Tilly, J.L. (1999). Targeted expression of Bcl-2 in mouse oocytes inhibits ovarian follicle atresia and prevents spontaneous and chemotherapy-induced oocyte apoptosis in vitro. Mol. Endocrinol. *13*, 841–850.

Patel, J., McLeod, L.E., Vries, R.G., Flynn, A., Wang, X., and Proud, C.G. (2002). Cellular stresses profoundly inhibit protein synthesis and modulate the states of phosphorylation of multiple translation factors. Eur. J. Biochem. *269*, 3076–3085.

Perez, G.I., Robles, R., Knudson, C.M., Flaws, J.A., Korsmeyer, S.J., and Tilly, J.L. (1999). Prolongation of ovarian lifespan into advanced chronological age by Bax-deficiency. Nat. Genet. *21*, 200–203.

Piñeiro, D., González, V.M., Hernández-Jiménez, M., Salinas, M., and Martín, M.E. (2007). Translation regulation after taxol treatment in NIH3T3 cells involves the elongation factor (eEF)2. Exp. Cell Res. *313*, 3694–3706.

Pru, J.K., and Tilly, J.L. (2001). Programmed cell death in the ovary: insights and future prospects using genetic technologies. Mol. Endocrinol. *15*, 845–853.

Ryazanov, A.G. (2002). Elongation factor-2 kinase and its newly discovered relatives. FEBS Lett. *514*, 26–29.

Ryazanov, A.G., Shestakova, E.A., and Natapov, P.G. (1988). Phosphorylation of elongation factor 2 by EF-2 kinase affects rate of translation. Nature *334*, 170–173.

Schedl, T., and Kimble, J. (1988). fog-2, a germ-line-specific sex determination gene required for hermaphrodite spermatogenesis in Caenorhabditis elegans. Genetics *119*, 43–61.

Stewart, J.B., Freyer, C., Elson, J.L., Wredenberg, A., Cansu, Z., Trifunovic, A., and Larsson, N.G. (2008). Strong purifying selection in transmission of mammalian mitochondrial DNA. PLoS Biol. *6*, e10.

Tilly, J.L. (2001). Commuting the death sentence: how oocytes strive to survive. Nat. Rev. Mol. Cell Biol. *2*, 838–848.

Timmons, L., and Fire, A. (1998). Specific interference by ingested dsRNA. Nature *395*, 854.

Titus, S., Li, F., Stobezki, R., Akula, K., Unsal, E., Jeong, K., Dickler, M., Robson, M., Moy, F., Goswami, S., et al. (2013). Impairment of BRCA1-related DNA double-strand break repair leads to ovarian aging in mice and humans. Sci. Transl. Med. *5*, 172ra121.

Wang, L., Du, F., and Wang, X. (2008). TNF-alpha induces two distinct caspase-8 activation pathways. Cell *133*, 693–703.

White, S.J., Kasman, L.M., Kelly, M.M., Lu, P., Spruill, L., McDermott, P.J., and Voelkel-Johnson, C. (2007). Doxorubicin generates a proapoptotic phenotype by phosphorylation of elongation factor 2. Free Radic. Biol. Med. *43*, 1313–1321.

Yuan, J., Shaham, S., Ledoux, S., Ellis, H.M., and Horvitz, H.R. (1993). The C. elegans cell death gene ced-3 encodes a protein similar to mammalian interleukin-1 beta-converting enzyme. Cell *75*, 641–652.